Cooperative Relative Localization for Moving UAVs with Single Link Range Measurements

Jared Strader, Yu Gu, Jason N. Gross, Matteo De Petrillo, Jeremy Hardy *West Virginia University*

***Abstract*—This paper describes a method for estimating the relative pose of a pair of unmanned aerial vehicles (UAV) using noisy measurements from ranging radios and each aircraft's on board navigation system. In this method, there is no prior information needed about the relative pose of each UAV. During the estimation of the relative pose of two traveling UAVs, only a single range measurement between UAVs is needed at each location. To augment this limited information, motion is used to construct a graph with the range measurements and displacement in position over multiple locations. First, the analytical solution is derived for the pose from the constructed graph assuming the system is free of noise. Then, the relative heading and bearing are estimated from noisy range measurements and the displacement in position using nonlinear least squares. The sensitivity to the geometry and measurement noise are then analyzed for various trajectories. For this paper, the problem is analyzed for the two-dimensional case where the UAVs are traveling at equal altitudes.**

***Keywords*—relative navigation; cooperative control; range-only measurements**

I. Introduction and Related Work

In applications involving multiple Unmanned Aerial Vehicles (UAV) such as formation flight, surveillance, cooperative control, and mapping, the relative pose between UAVs provides vital information for coordinating effectively. In formation flight, the follower is controlled based on the relative position of the leader. For localization and mapping, the transformation between each UAVs reference frame is necessary to fuse information to construct a map of the environment. In the case GPS is not available, each UAV must rely relative sensor measurements in order to navigate in a common frame of reference. The majority of distributed estimation tasks require the ability to transform measurements between reference frames for each UAV. In [1], a relative navigation filter is developed to enable target hand-off in a GPS-denied environment, but in order to run the filter, the transformation between reference frames is required to initialize the filter. In many cases, UAVs may rely on sensors that only provide range measurements between UAVs due to environmental or hardware constraints. More importantly, the majority of work on localization either require stationary landmarks or are not limited to range only measurements. Localization using range only measurements has been studied extensively for static sensor networks [2]. Several algorithms have been proposed for determining the relative position of each node; however, wireless sensor networks consist of many stationary nodes, and the relative orientation is not of interest in these algorithms. Localization for mobile robots in two dimensions using range only measurements have been demonstrated in [3], [4], [5]. In these works, the robots travel through a sequence of random positions and orientations, and the relative position between robots is determined using range only measurements. The problem presented in this work is similar to the problem presented in [3], [4], [5], but in contrast, this work presents a method for determining the relative position and orientation using coordinated motion rather than arbitrary motion. Specifically, we show that when two UAVs travel at constant velocity there are at most four solutions for the relative pose after collecting three range measurements. In addition, the total number of solutions are reduced to obtain a single unique solution with one additional measurement by performing a single maneuver. For certain trajectories, the relative pose may have less than three solutions after three measurements or the solution may be indeterminate. To verify the algorithm, an estimation algorithm is presented for estimating all the solutions and obtaining a single unique solution using cooperative control. In addition, Monte Carlo simulations are completed to analyze the sensitivity to geometry and measurement noise.

II. Problem Formulation

In this paper, we consider two UAVs, platform A and platform B. Initially, each platform moves at a constant velocity through a sequence of positions $\{A_1, A_2, ..., A_n\}$ for platform A and $\{B_1, B_2, ..., B_n\}$ for platform B. At each of these locations, both platforms measure the distance between platforms $\{d_1, d_2, ..., d_n\}$. In addition, the displacement in position between locations for each platform is measured using each platform's on board navigation system. The displacement in position between locations will be denoted as $\{d_{A,1}, d_{A,2}, d_{A,n-1}\}$ for platform A and $\{d_{B,1}, d_{B,2}, d_{B,n-1}\}$ for platform B where n is the total number of locations. Note that the displacement in position between locations will be referred to as simply the displacement. Since the displacement is not dependent on the reference frame, the displacement can be exchanged between platforms. Note the particular method for determining the displacement does not affect the solution for this problem since the displacement is not dependent on the reference frame. The trajectory for platform A and platform B after traveling through three locations is presented in Fig. 1. In this paper, we consider the scenario of determining the relative pose of platform B in polar coordinates with respect to platform A. The relative bearing of platform B is denoted by ϕ_B and the radial coordinate of platform B is denoted by r_B. The formulation presented in this work is equivalent when determining the relative position of platform A with respect to platform B.

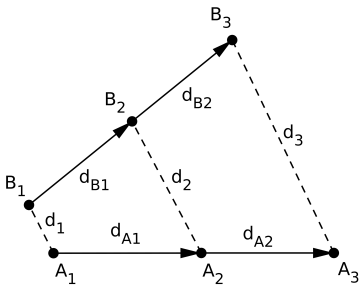

Fig. 1. Trajectories of platforms A and B for three positions. The position of each platform is denoted by $A_1, A_2, ..., A_n$ for platform A and $B_1, B_2, ..., B_n$ for platform B where n is the total number of locations. The displacement in distance between locations is denoted as $d_{A,1}, d_{A,2}, d_{A,n-1}$ for platform A and $d_{B,1}, d_{B,2}, d_{B,n-1}$ for platform B

III. Analytical Solutions with Three Range Measurements

A. Connection to Mechanical Linkages

If each platform travels at a constant velocity, the arrangement of distance measurements is analogous to a mechanical linkage. At constant velocity, the path between locations is straight, so the trajectories of each platform can be modeled as rigid links with length equal to the displacement in position between locations. These links are represented by $\{d_{A,1}, d_{A,2}, d_{A,n-1}\}$ for platform A and $\{d_{B,1}, d_{B,2}, d_{B,n-1}\}$ for platform B. In addition, the range between platforms at each location can be modeled as rigid links. These links are represented by the range measurements $\{d_1, d_2, ..., d_n\}$. At each location, the links are connected by the position of both platforms, which are modeled as revolute joints. The number of joints and links in this linkage are determined by the number of locations. For any number of locations, the length of each link is known from the displacement in position and the range between platforms. The goal is to solve for the orientation of the each link with respect to the fixed link since this will provide the relative pose between platforms at each location. To determine the orientation of each link without prior information, the linkage must be a rigid structure. Using the *Kutzbach criterion*, the mobility, M, can be obtained for any number of measurements given the number of links n, the number of single degree of freedom joints j_1, and the number of two degree of freedom joints, j_2. The *Kutzbach criterion* as defined in [7] is

$$M = 3(n-1) - 2j_1 - j_2. \tag{1}$$

If each platform travels through two locations and obtains a measurement at each location, the linkage will consist of four revolute joints and four links in total to form a four bar mechanism. Considering the *Kutzbach criterion* for this four bar mechanism, this linkage consists of a single degree of freedom. This means that the configuration of the linkage is defined by a single parameter in addition to the link lengths [7], and the linkage is indeterminate without the prior knowledge of the orientation of one of the free links. If each platform travels through three locations and obtains a measurement at each location, the linkage will consist of six revolute joints and seven links in total to form a seven bar mechanism. Since the platforms are traveling at constant velocity, the links representing the displacement can be combined to form a single rigid link for each platform. This means the number of links in the linkage is reduced from seven links to five links, so the linkage will consist of six revolute joints and five links in total to form a five bar linkage. Considering *Kutzbach criterion* for this five bar mechanism, this linkage consists of zero degrees of freedom. This means the linkage is a rigid structure, so prior information about the orientation of the links is not needed to solve for the configuration given the length of each link. This is roughly equivalent to adding a single rigid link between the fixed link and coupler in a four bar mechanism. Although prior information is not needed to solve for the configuration of the linkage, this does not mean there is a single solution for the linkage. The linkage may be constructed in multiple different configurations, but each configuration can be obtained independently from the link lengths.

Using this analogy, the relative position of B with respect to A can be obtained by solving the loop closure equations of the five bar linkage formed from the displacement in position, distance between platforms, and the locations of platform A and platform B. We define each link as a vector defined by the link length $r_1 = d_{A1}+d_{A2}$, $r_2 = d_3$, $r_3 = d_{B1}+d_{B2}$, $r_4 = d_1$, and $r_5 = d_2$, and the angle between the horizontal axis and the link θ_1, θ_2, θ_3, θ_4, and θ_5. The linkage constructed from the trajectories of platform A and platform B is presented in Fig. 2. Since the goal is to obtain the relative position of platform B with respect to platform A, the displacement in position of platform A, r_1, is set as the fixed link, so the angle of each link is relative to r_1. This means the linkage is constructed in the inertial frame of platform A. Note θ_1 is not presented in Fig. 2 because the free links are relative to the fixed link, r_1.

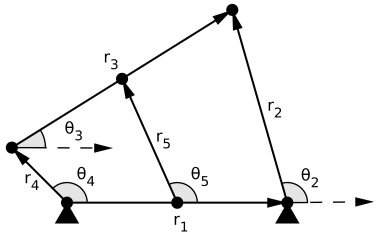

Fig. 2. Single configuration of 5 bar linkage constructed from the UAV trajectories for 3 locations where $r_1 = d_{A1} + d_{A2}$, $r_2 = d_3$, $r_3 = d_{B1} + d_{B2}$, $r_4 = d_1$, and $r_5 = d_2$. Note θ_1 is not displayed because $\theta_1 = 0$.

B. Finding θ_3

The loop closure equations for the linkage in vector form are defined by (2) and (3).

$$\vec{r_1} + \vec{r_2} = \frac{d_{A1}}{r_1}\vec{r_1} + \frac{d_{B2}}{r_3}\vec{r_3} + \vec{r_5} \tag{2}$$

$$\frac{d_{A1}}{r_1}\vec{r_1} + \vec{r_5} = \frac{d_{B1}}{r_3}\vec{r_3} + \vec{r_4} \tag{3}$$

Equations (2) and (3) can be rearranged and separated in real and imaginary components in (4) and (5).

$$\begin{aligned} i&: r_2 \sin\theta_2 = r_5 \sin\theta_5 + d_{B2} \sin\theta_3 + d_{A2} \sin\theta_1 \\ j&: r_2 \cos\theta_2 = r_5 \cos\theta_5 + d_{B2} \cos\theta_3 + d_{A2} \cos\theta_1 \end{aligned} \tag{4}$$

$$\begin{aligned} i&: r_4 \sin\theta_4 = r_5 \sin\theta_5 - d_{B1} \sin\theta_3 + d_{A1} \sin\theta_1 \\ j&: r_4 \cos\theta_4 = r_5 \cos\theta_5 - d_{B1} \cos\theta_3 + d_{A1} \cos\theta_1 \end{aligned} \tag{5}$$

Since the links are relative to r_1, the angle of r_1 does not change the outcome of the solution, so any angle can be chosen for θ_1. If the real and imaginary parts of (4) and (5) are squared and summed, θ_2 can be eliminated from (4) and θ_4 can be eliminated from (5) using the Pythagorean trigonometric identity given by $\sin\theta^2 + \cos\theta^2 = 1$. Letting $\theta_1 = \pi/2$, (4) and (5) can be reduced to (6) and (7).

$$\begin{aligned} r_2^2 = r_5^2 + r_5(2d_{B2} \sin\theta_3 \sin\theta_5 + 2d_{B2} \cos\theta_3 \cos\theta_5 \\ - 2d_{A2} \sin\theta_5) - 2d_{A2} d_{B2} \sin\theta_3 - d_{A2}^2 + d_{B2}^2 \end{aligned} \tag{6}$$

$$\begin{aligned} r_4^2 = r_5^2 - r_5(2d_{B1} \sin\theta_3 \sin\theta_5 + 2d_{B1} \cos\theta_3 \cos\theta_5 \\ - 2d_{A1} \sin\theta_5) - 2d_{A1} d_{B1} \sin\theta_3 + d_{A1}^2 + d_{B1}^2 \end{aligned} \tag{7}$$

If platform A and platform B are moving at a constant speed, $d_{A1} = d_{A2} = d_A$ and $d_{B1} = d_{B2} = d_B$. Substituting these values and combining (6) and (7), a single equation is obtained for θ_3 as a function of the link lengths.

$$r_2^2 + r_4^2 = 2r_5^2 - 4d_A d_B \sin\theta_3 + 2d_A^2 + 2d_B^2 \tag{8}$$

Equation (8) can be rearranged to obtain a more simple solution. Let $r_a = -4d_A d_B$ and $r_b = r_2^2 + r_4^2 - 2r_5^2 - 2d_A^2 - 2d_B^2$. Substituting r_a and r_b in (8), the following equations are obtained for the $\sin\theta_3$ when $\theta_1 = \pi/2$ and for the $\cos\theta_3$ when $\theta_1 = 0$

$$r_a \sin\theta_3 = r_b \tag{9}$$

$$r_a \cos\theta_3 = r_b \tag{10}$$

The angle between the trajectories of platform A and platform B, θ_3, has a single unique solution where $0 \leq \theta_3 \leq \pi$. Note that the angle between trajectories is not equal to the relative orientation. The relative orientation is equal in magnitude to the angle between trajectories, but the angle between trajectories is always positive, so $\theta_B = \pm\theta_3$. The potential solutions for θ_2 can be obtained using the result of θ_3, but the solutions for θ_2 must be reflected across the path of platform A.

C. Finding θ_2

Consider the following loop closure equation of the linkage presented in Fig. 2 defined by (11).

$$\vec{r_1} + \vec{r_2} = \vec{r_3} + \vec{r_4} \tag{11}$$

Similar to the derivation for θ_3, (11) can be rearranged and separated into real and imaginary components.

$$\begin{aligned} i&: r_4 \sin\theta_4 = r_1 \sin\theta_1 + r_2 \sin\theta_2 - r_3 \sin\theta_3 \\ j&: r_4 \cos\theta_4 = r_1 \cos\theta_1 + r_2 \cos\theta_2 - r_3 \cos\theta_3 \end{aligned} \tag{12}$$

Since θ_1 and θ_3 are known values, the constants u and v can be defined as

$$\begin{aligned} u &= r_1 \sin\theta_1 - r_3 \sin\theta_3 \\ v &= r_1 \cos\theta_1 - r_3 \cos\theta_3. \end{aligned}$$

Then, the real and imaginary parts of (12) can be squared and summed to obtain (13).

$$r_4^2 - r_2^2 - u^2 - v^2 = 2ur_2 \sin\theta_2 - 2vr_2 \cos\theta_2 \tag{13}$$

Equation 13 has the form $a \sin\theta_2 + b \cos\theta_2 = c$, where

$$\begin{aligned} a &= 2ur_2 \\ b &= -2vr_2 \\ c &= -r_2^2 + r_4^2 - u^2 - v^2. \end{aligned}$$

Equation 13 can be written in terms of tangent instead of sine and cosine by substituting the half-angle formulas to obtain sine and cosine in terms of tangent of the half angle. If $t = \tan\theta_2/2$, then $\sin\theta_2 = 2t/(1+t^2)$ and $\cos\theta_2 = (1-t^2)/(1+t^2)$. After substituting θ_3, we obtain the following equations for t

$$\alpha t^2 + \beta t + \gamma = 0 \tag{14}$$

where $\alpha = -b - c$, $\beta = 2a$, and $\gamma = b - c$. The same process can be completed to obtain solutions for θ_4 and θ_5. Although these equations are second order polynomials, the solutions can be reflected on either side of the straight line trajectory of platform A, so at least 4 solutions exist for θ_2, θ_4, and θ_5. Since the relative position is completely defined by r_2 and θ_2, it is only necessary to estimate θ_2 and θ_3. Note that θ_2 is a function of θ_3 and the distance measurements, $\theta_2 = f(d_1, d_2, d_3, \theta_3)$ and θ_3 is only a function of the distance measurements, $\theta_3 = f(d_1, d_2, d_3)$. Since the velocity is constant, the terms d_A and d_B are constant.

IV. Estimating the Relative Pose with Noise

If the system is free of noise, the four possible solutions of the relative position can simply be obtained by plugging in the necessary values in (10) and (14) to obtain the solutions in polar coordinates. Since the measurements of the range between platforms and the displacement in position are both noisy, the system may be inaccurate or unsolvable depending on the magnitude of the noise and the geometry of the trajectories. Since the platforms are traveling at a constant velocity, the angle between the trajectories, θ_3, is constant over any number of time steps. Due to this, a system of equations for θ_3 can be formed where n is the number of observations.

$$\begin{bmatrix} r_a(d_1, d_2, d_3) \\ r_a(d_2, d_3, d_4) \\ . \\ . \\ r_a(d_{n-2}, d_{n-1}, d_n) \end{bmatrix} \sin\theta_3 = \begin{bmatrix} r_b(d_1, d_2, d_3) \\ r_b(d_2, d_3, d_4) \\ . \\ . \\ r_b(d_{n-2}, d_{n-1}, d_n) \end{bmatrix} \tag{15}$$

Using linear least squares, a batch estimate of θ_3 can be performed using multiple observations. Note that each observation includes three measurements, so the relative position cannot be estimated without at least three observations. For

example, observation at time step k includes measurements from k, $k-1$, and $k-2$. The sensitivity to geometry and noise for θ_3 will be discussed in the results section. Since the distance between platforms is measured directly, only the relative bearing of platform B must be estimated using (14). Using the quadratic equation, each of the four solutions can be determined using nonlinear least squares to estimate $t = \tan\theta_2/2$.

$$2\alpha t = -\beta \pm \sqrt{\beta^2 - 4\alpha\gamma} \tag{16}$$

Note α, β, and γ are all functions of θ_3 in addition to the link lengths, so θ_3 must be estimated prior to estimating θ_2. Since the relative bearing changes at each time step, a batch estimate of the relative bearing may only be performed at certain geometries. Since the formulation is sensitive to noise, the solutions are smoothed using exponential smoothing. In the case $\beta^2 - 4\alpha\gamma < 0$, additional measurements can be obtained to solve for the relative bearing.

V. Reducing the Number of Solutions

After traveling through three locations, there are four possible solutions for the relative position of platform B, two solutions for relative bearing for each of the two solutions for the relative orientation. To find the correct solution, cooperative control is used to assign weights to each solution. After obtaining each of the four solutions, the relative pose and velocity for each of the four solutions for platform B are stored in memory, and platform A turns to a different heading. At this point, the position of platform B in Cartesian coordinates, $(\hat{x}_{B,k}, \hat{y}_{B,k})$, will be propagated using the most recent estimates for each of the four solutions.

$$\hat{x}_{B,k+1} = \hat{x}_{B,k} + \dot{x}_{B,k}dt \tag{17}$$

$$\hat{y}_{B,k+1} = \hat{y}_{B,k} + \dot{y}_{B,k}dt \tag{18}$$

Note that if platform B exchanges position and velocity information instead of only range information, the coordinate frame transformation may be calculated for each of the four solutions, and the position may be propagated using the navigation system on board platform B. In the case this information is not available, the position and velocity can be obtained from the constructed linkage for each solution. To determine the weights for each solution, the expected distance between platforms for each solution is calculated using the propagated position of platform B. Let $\hat{d}_{i,k}$ be the expected distance for the ith solution at time step k where $(\hat{x}_{A,k}, \hat{y}_{A,k})$ and $(\hat{x}_{B,k}, \hat{y}_{B,k})$ are the position in Cartesian coordinates for platform A and platform B, respectively.

$$\hat{d}_k = \sqrt{(\hat{x}_{A,k} - \hat{x}_{B,k})^2 + (\hat{y}_{A,k} - \hat{y}_{B,k})^2} \tag{19}$$

Then, the residual distance, $\tilde{d}$, at time step k can be calculated using the difference in the expected distance and the range measurement.

$$\tilde{d}_k = \hat{d}_k - d_k \tag{20}$$

If the system is free of noise, $\tilde{d} = 0$ for the true solution and $\tilde{d} \neq 0$ for false solutions. The weights for each solution are assigned as the inverse of the residual distance.

$$w = \frac{1}{\tilde{d}_k} \tag{21}$$

If the system is free of noise, (21) approaches infinity for the correct solution. In practice, the weight with the highest value is chosen as the best solution.

VI. Special Cases

Depending on the geometry of the trajectories, the number of possible solutions and singularity of θ_2 may vary. When the platforms are traveling at constant velocity, there are only four possible cases for the geometry. The platforms must be either be traveling along the same line, traveling along parallel lines with equal velocity, traveling along parallel lines with different velocity, or traveling along intersecting lines. If the platforms are traveling along intersecting lines, there are at most four solutions for the relative position regardless of the velocity of each platform. For each case, the number of solutions for the relative position are different, but there are at most two solutions for the relative orientation in each case. Each case is easily detectable using the relationships between the displacement in position and the range between platforms. The solutions for each case are discussed in this section.

A. Same Line

If the platforms are traveling along the same line in opposite directions there exists a single unique solution for the position and a single unique solution for the relative orientation. This is detectable by comparing the magnitude of the velocity vectors and the change in distance measurements between time steps. When the platforms are traveling in opposite directions along the same line, then

$$d_{A1} + d_{B1} = |d_1 - d_2| \tag{22}$$

$$d_{A2} + d_{B2} = |d_2 - d_3| \tag{23}$$

Note that d_1, d_2, and d_3 are measurements of the distance between platforms and d_A and d_B are the displacement in position for platform A and platform B, respectively. The absolute value is necessary because $d_1 - d_2 > 0$ and $d_2 - d_3 > 0$ when the platforms are traveling towards each other and $d_1 - d_2 < 0$ and $d_2 - d_3 < 0$ when the platforms are traveling away from each other. An illustration of this case is presented in Fig. 3 for when the platforms are traveling along the same line towards each other. If the platforms are traveling in the same direction, then $d_1 - d_2 = 0$ and $d_2 - d_3 = 0$, and there are an infinite number of solutions. This situation is discussed in the following section. In the case the platforms are not traveling along the same line, the change in the distance measurement between platforms will always be less than the sum of the distance traveled by each platform.

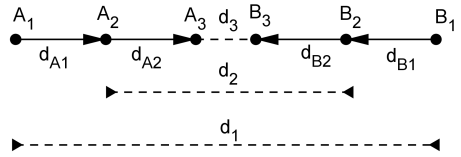

Fig. 3. Path of platform A and platform B when the platforms are traveling towards each other.

B. Parallel with Equal Velocities

If the platforms are traveling parallel with equal velocities, there are infinite solutions for the relative position and a single unique solution for the relative orientation. An illustration of this case is presented in Fig. 4. In this case, we have

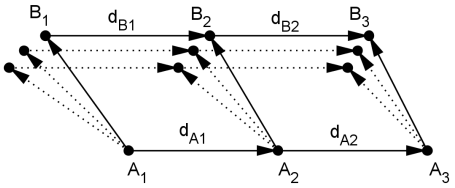

Fig. 4. Path of platform A and platform B the platforms are traveling parallel with equal velocities. In this case, $\theta_3 = 0$, $d_{A1} = d_{A2} = d_{B1} = d_{B2}$, and $d_1 = d_2 = d_3$, so in (10) and (14), $r_2 = r_4 = r_5$ and $r_1 = r_2$.

$d_{A1} = d_{A2} = d_{B1} = d_{B2}$, $r_2 = r_4 = r_5$ and $r_1 = r_3$. If we substitute these values in (10), then $\cos\theta_3 = 1$. Then, $\theta_1 = \theta_3 = 0$, so substituting these values in (14) causes the constants to equal zero. Therefore, θ_2 is indeterminate because $(0)t_2^2 + (0)t_2 + (0) = 0$ when the platforms are traveling parallel with equal velocities. This can easily be visualized from the constructed linkage. In this case, the linkage forms a parallelogram structure, so the link formed by the displacement in position of platform B can rotate through an infinite number of positions.

C. Parallel with Different Velocities

If the platforms are traveling parallel at different speeds, there are two unique solutions for the relative position and a single unique solution for the relative orientation. In this case, $\theta_1 = 0$ and $\theta_3 = 0$ because the platform are traveling parallel. By substituting $\theta_1 = 0$ and $\theta_3 = 0$ into (14), $\beta = 4r_1r_2\sin\theta_1 - 4r_2r_3\sin\theta_3 = 0$, so (14) becomes

$$\alpha t^2 + \gamma = 0 \tag{24}$$

Note $\alpha \neq 0$ and $\gamma \neq 0$ if both platforms are in motion and are traveling at different velocities. Equation (24) has two solutions, which are equal in magnitude but have opposite signs. The solutions to (24) and the reflection are equivalent, so there are only two solutions for the relative position when the platforms are traveling parallel with different velocities. An illustration of this case is presented in Fig. 5.

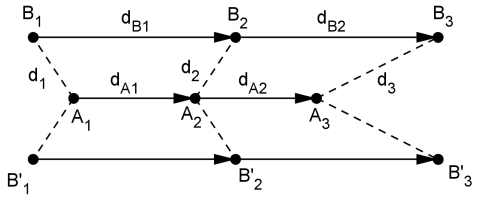

Fig. 5. Path of platform A and platform B when platforms are traveling parallel with different velocities. In this case, $\theta_3 = 0$, $d_{A1} + d_{A2} \neq d_{B1} + d_{B2}$.

D. Intersecting Lines

If the platforms are not traveling parallel and are not traveling along the same line, there are four unique solutions for the relative position and two unique solutions for the relative orientation. In this case, $\theta_3 \neq 0$, so there are two solutions for the relative orientation. Equation (14) has two solutions when the $\theta_3 \neq 0$, and this solution may be reflected across the path of platform A to account for the position and negative solution of the relative orientation. An illustration of this case is presented in Fig. 6. Notice the first and second solution are for the positive relative orientation. The solutions for the negative relative orientation are reflected across the path of platform A to form the third and fourth solutions.

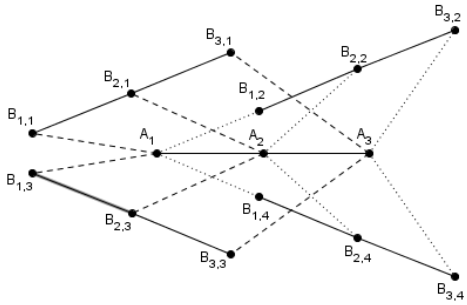

Fig. 6. Path of platform A and platform B when platforms are traveling along intersecting lines. In this case, $\theta_3 \neq 0$, and there are two solutions for the relative orientation and four solutions for the relative position. The solutions for the relative position of platform B are given by $B_{i,j}$ where i is the location number and j is the solution number.

VII. Simulation Results

We consider here only the case where the platforms are traveling along intersecting lines, as the other three cases are not difficult to detect and are not as likely in most scenarios. The simulations were performed by adding zero mean Gaussian noise to the distance measurements between platforms the displacement in position between locations. In performing various simulations, the goal is to verify the algorithm and analyze the sensitivity to different parameters. The first experiment consists of a single path for platform A and platform B. In this experiment, the platforms start in different locations 150 meters apart. The distance intervals d_A and d_B between observations is varied to analyze the sensitivity to this parameter while the level of noise in the ranging

measurement and displacement are both held constant. The level of ranging error for displacement has a standard deviation between 1.7% the total displacement, which is based on the typical performance of current visual odometry algorithms [8], [9], [10], [11]. The average root mean square error (RMSE) for the relative heading and relative bearing is presented in Fig. 7 for 100 Monte Carlo trials for each distance interval. As the distance interval increases, the error in both the relative heading and relative bearing decrease. This is likely due to the effect of the distance interval on the ratio of the displacement in position to the distance between platforms, r_2/r_1. If r_2/r_1 is small, the number of observation included in the least squares estimate has little effect on the accuracy. This means that only a few measurements are necessary to obtain an accurate estimate if r_2/r_1 is small. If the platforms are far away from each other, the time between observations must be increased to obtain a larger distance interval and lower r_2/r_1, so each platform must travel a straight line path for a longer amount of time if the platforms are far away from each other. In the case the platforms are flying in directions which increase the ratio over time, the batch size can be increased to reduce drift and variance by using additional observations when r_2/r_1 is small. Note that r_2/r_1 always increases over time if the platforms are traveling away from each other. This is because the distance interval remains constant while the distance between platforms increase. Since the platforms are required to travel at constant velocity for this method, r_2/r_1 is guaranteed to increase if the platforms are traveling away from each other. This issue can be mitigated by performing a batch estimate which includes observations when r_2/r_1 is small. Since r_2/r_1 is dependent on the distance interval, similar performance can be obtained at large distances by increasing the distance interval to reduce r_2/r_1. The cumulative distribution function (CDF) for the trials are presented in Fig. 8.

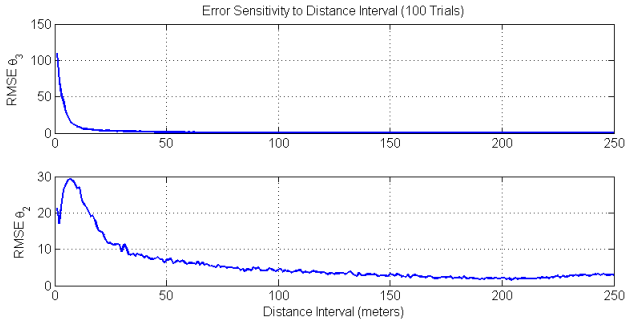

Fig. 7. Average RMSE for the relative heading and relative bearing of platform B. The horizontal axis is the distance interval, and the vertical axis is the average RMSE error. 100 trials were completed for each distance interval.

In the next experiment, the distance interval is held constant at 25 meters. The level of noise in the ranging measurement is held constant with a standard deviation of 0.05 meters, and the level of noise in the displacement in position is held constant at 1.7% the displacement. The flight path is varied by changing the heading of platform B with respect to platform A to analyze the sensitivity to flight path geometry. The RMSE

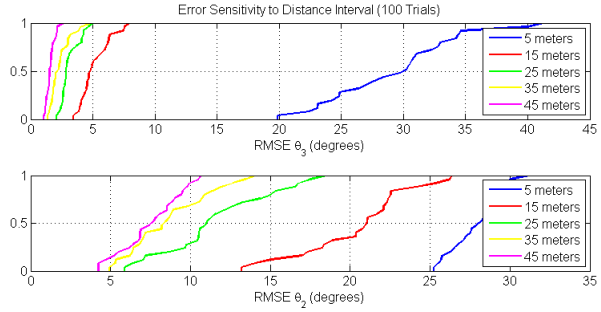

Fig. 8. CDF of the relative heading and relative bearing of platform B with respect to platform A for various distance intervals. 100 trials were completed for each distance interval.

of the relative heading and relative bearing are presented in Fig. 9. The error for the relative heading is greatest when the platform trajectories are nearly parallel. Although a parallel configuration is detectable from the distance measurements, the error in the relative position is still greatest in this configuration. The CDF for the trials are presented in Fig. 10. The performance is similar for the platforms when the trajectories are not near parallel with less than 1 degree error for the relative heading and less than 5 degrees error for the relative bearing in 100% of the trials at 45, 90, and 135 degrees for the relative heading, but the performance decreases quickly as the relative heading approaches 0 and 180 degrees.

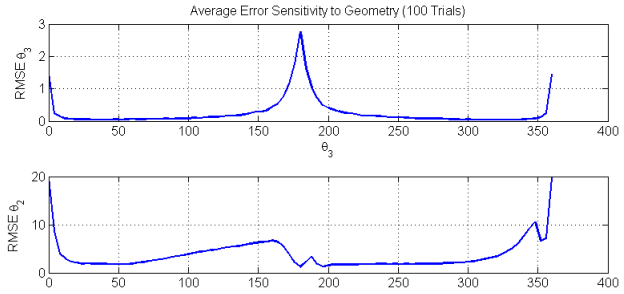

Fig. 9. Average RMSE for the relative heading and relative bearing of platform B. The horizontal axis is the relative heading of platform B, and the vertical axis is the average RMSE error. 100 trials were completed for each relative heading of platform B.

In the next experiment, the distance interval is held constant at 25 meters, and the geometry is held constant with the relative heading of platform B at 0 degrees. The level of noise for the ranging measurement is varied based on high and low quality ranging sensors. The level of noise for the displacement in position is held constant with a standard deviation of 1.7% of the displacement. The RMSE of the relative heading and relative bearing are presented in Fig. 11. The CDF for the trials are presented in 12.

In the next experiment, the distance interval is held constant at 25 meters, and the geometry is held constant with the relative heading of platform B at 0 degrees. The standard deviation for the displacement in position is varied between

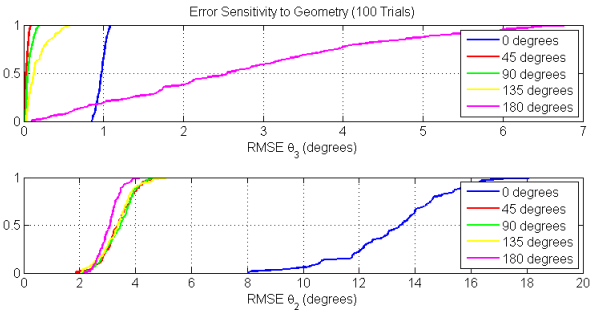

Fig. 10. CDF of the relative heading and relative bearing of platform B with respect to platform A for various relative headings of platform B. 100 trials were completed for each relative heading of platform B.

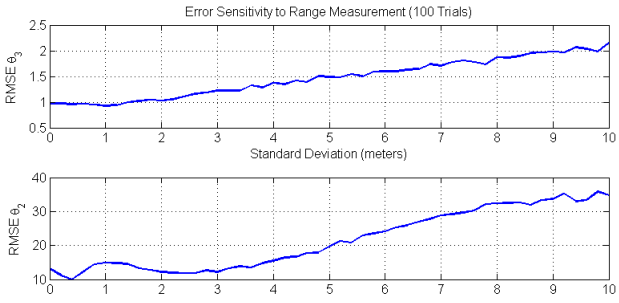

Fig. 11. Average RMSE for the relative heading and relative bearing of platform B. The horizontal axis is the standard deviation of ranging measurements between platforms, and the vertical axis is the average RMSE error. 100 trials were completed for each level of ranging error.

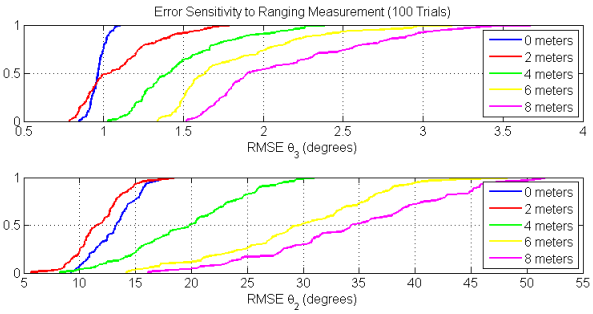

Fig. 12. CDF of the relative heading and relative bearing of platform B with respect to platform A for various levels of error for the ranging measurements between platforms. 100 trials were completed for each level of ranging error.

1% and 5%. The level of noise for the ranging measurements is held constant with a standard deviation of 0.05 meters. The RMSE of the relative heading and relative bearing are presented in Fig. 13. The CDF for the trials are presented in 14.

In the last experiment, the reduction of solutions is analyzed for various geometries and noise levels. The objective of this experiment is to verify the validity of the algorithm for reducing the number of solutions. The distance interval is held constant at 25 meters for this experiment, but the geometry and initial position of each platform are varied for each simulation.

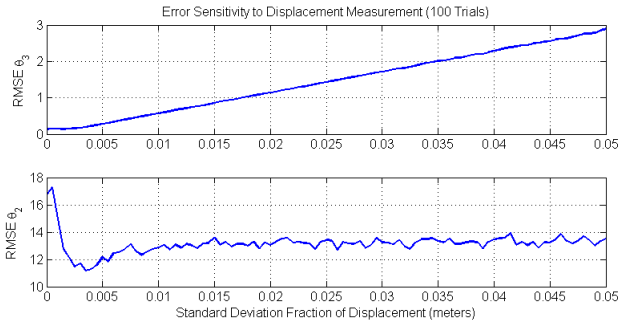

Fig. 13. Average RMSE for the relative heading and relative bearing of platform B. The horizontal axis is the standard deviation as a fraction of the total displacement between locations. 100 trials were completed for each level of displacement error. Note the error is shown as the percentage of the displacement.

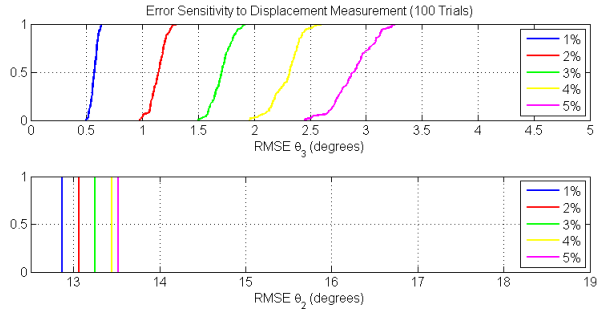

Fig. 14. CDF of the relative heading and relative bearing of platform B with respect to platform A for various levels of error for the displacement in position between locations. 100 trials were completed for each level of of displacement error. Note the standard deviation of the displacement are shown as a percent of the total displacement.

The starting position of each platform is chosen as random according to a uniform distribution within a 1000 by 1000 meters square.

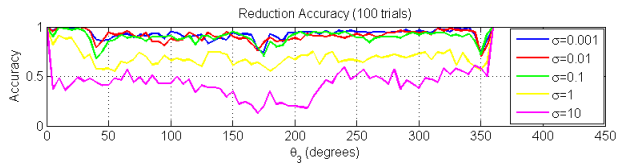

Fig. 15. Percentage of trials that successfully predicted the correct solution for various levels of error for the ranging error. The horizontal axis is the heading of platform B and the vertical axis is the percentage of trials that successfully predicted the correct solution.

As seen in Fig. 16, the relative heading of platform B does not affect the accuracy of predicting the correct solution except when the platforms are traveling parallel. In this case, the correct solution is predicted in 100% of trials. When the platforms are not traveling parallel, the level of error in the ranging measurements and displacement in position greatly affect the outcome of the algorithm. If the error is too large, the algorithm may predict the incorrect solution. This is due to the fact that the residual distance is calculated by propagating the position obtained from relative bearing. If the error in the

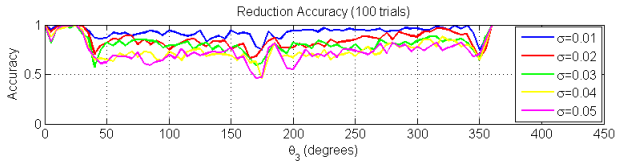

Fig. 16. Percentage of trials that successfully predicted the correct solution for various levels of error for the displacement error. The horizontal axis is the heading of platform B and the vertical axis is the percentage of trials that successfully predicted the correct solution.

relative bearing is too large, the residual distance may not be accurate, which results in a false detection of the correct solution.

VIII. Conclusion and Future Work

This paper presents an algorithm for estimating the relative pose between moving UAVs using range only measurements and analyzes the sensitivity to flight geometry, observation frequency, and measurement noise. The algorithm is only dependent on measuring the distance between UAVs and the displacement in position between measurement observations. The specific method for estimating the displacement in position does not affect the algorithm. To analyze the effectiveness, several simulations were completed varying the observation frequency, geometry, and measurement noise. The simulations show that the frequency of observation impacts the performance more than the geometry or the amount of error in the distance measurements. From the simulation, the geometry seems to not have a significant impact on the performance. Future work will include developing a system for experimental testing and investigating strategies for reducing the uncertainty in the estimation algorithm.

Acknowledgment

This material is based upon work supported by the United States Air Force under Contract No. FA8650-15-M-1943.

References

[1] J. Hardy, J. Strader, J. N. Gross, Y. Gu, M. Keck, J. Douglas, C. N. Taylor, "Unmanned Aerial Vehicle Relative Navigation in GPS Denied Environments" in Proceedings of IEEE/ION Position Localization and Navigation Symposium. IEEE/ION, 2016.

[2] Wang, Jing, Ratan K. Ghosh, and Sajal K. Das. "A survey on sensor localization." Journal of Control Theory and Applications 8.1 (2010): 2-11.

[3] Zhou, Xun S., and Stergios Roumeliotis. "Robot-to-robot relative pose estimation from range measurements." Robotics, IEEE Transactions on 24.6 (2008): 1379-1393.

[4] Trawny, Nikolas, and Stergios Roumeliotis. "On the global optimum of planar, range-based robot-to-robot relative pose estimation." Robotics and Automation (ICRA), 2010 IEEE International Conference on. IEEE, 2010.

[5] Shames, Iman, et al. "Cooperative self-localization of mobile agents." Aerospace and Electronic Systems, IEEE Transactions on 47.3 (2011): 1926-1947.

[6] Cornejo, Alejandro, and Radhika Nagpal. "Distributed Range-Based Relative Localization of Robot Swarms." Algorithmic Foundations of Robotics XI. Springer International Publishing, 2015. 91-107.

[7] J. J. Uicker, G. R. Pennock, and J. E. Shigley, 2003, Theory of Machines and Mechanisms, Oxford University Press, New York.

[8] Reuben Strydom, Saul Thurrowgood, and Mandyam V Srinivasan. "Visual odometry: Autonomous uav navigation using optic flow and stereo." In Australasian Conference on Robotics and Automation (ACRA), pages 110. Australian Robotics and Automation Association, 2014.

[9] Roger-Verdeguer, Jose F., Mikael Mannberg, and Al Savvaris. "Visual odometry with failure detection for the aegis UAV." Imaging Systems and Techniques (IST), 2012 IEEE International Conference on. IEEE, 2012.

[10] Mouats, Tarek, et al. "Thermal Stereo Odometry for UAVs." Sensors Journal, IEEE 15.11 (2015): 6335-6347.

[11] Warren, Michael, Peter Corke, and Ben Upcroft. "Long-range stereo visual odometry for extended altitude flight of unmanned aerial vehicles." The International Journal of Robotics Research (2015): 0278364915581194.